

# Downside Up: Rethinking Parcel Position for Aerial Delivery

Przemyslaw M. Kornatowski , Mir Feroskhan , William J. Stewart , and Dario Floreano , *Senior Member, IEEE*

**Abstract**—The conventional approach to parcel placement in most delivery drone designs today is to place the parcel centrally beneath the drone’s rotor plane. However, if the parcel is too large, this will result in an obstruction of the propeller slipstream, incurring significant drag. As such, the parcel’s location below the rotor plane limits the size of parcels that can be delivered, specifically super-sized parcels that protrude beyond the bounds of the four rotors. Delivering these large parcels requires bigger drone platforms, which consequently consume more energy, necessitate large storage spaces, and are less portable. In this letter, we propose an alternative approach, placing the parcel above the rotor plane. However, placing a parcel above a quadcopter encounters two main challenges. The first is the optimal position of the CG to maintain stability of the drone. Second is the aerodynamic influence on the lift of the drone with a parcel is placed above the propellers. To address these challenges, aerodynamic characterization experiments were performed and a new drone design was proposed. This letter presents a prototype quadcopter design solution that places the parcel above the propellers to enable delivery of super-sized parcels, as well as a compact rotor design configuration for lower storage cost and increased portability. The new approach of placing an over-sized parcel above propellers provides the 82% increase in thrust over putting the parcel below the propellers.

**Index Terms**—Aerial systems, applications, intelligent transportation systems, unmanned aerial vehicles.

## I. INTRODUCTION

**D**RONES are increasingly becoming a useful tool adopted by logistics companies as a delivery solution that is economical, environmentally friendly, and efficient [1]. Threats to urban sustainability such as traffic congestion, living-space constraints and air pollution further propel the need to re-examine conventional dispatch services amidst the growing expectations of e-commerce patrons [2]. Several notable logistics companies have already begun drone deliveries of commercial goods such

Manuscript received November 11, 2019; accepted April 15, 2020. Date of publication May 11, 2020; date of current version June 1, 2020. This letter was recommended for publication by Editor Jonathan Roberts upon evaluation of the Associate Editor and Reviewers’ comments. This work was supported by the Swiss National Science Foundation through the National Centre of Competence in Research (NCCR) Robotics and armasuisse. (*Corresponding author: Przemyslaw M. Kornatowski.*)

Przemyslaw M. Kornatowski, William J. Stewart, and Dario Floreano are with the Laboratory of Intelligent Systems, School of Engineering, Ecole Polytechnique Federale de Lausanne, Lausanne CH1015, Switzerland (e-mail: przemyslaw.kornatowski@epfl.ch; william.stewart@epfl.ch; dario.floreano@epfl.ch).

Mir Feroskhan is with the School of Mechanical and Aerospace Engineering, Nanyang Technological University, Singapore 639798, Singapore (e-mail: mir.feroskhan@ntu.edu.sg).

This article has supplementary downloadable material available at <http://ieeexplore.ieee.org>, provided by the authors.

Digital Object Identifier 10.1109/LRA.2020.2993768

as Amazon.com, Alibaba, Dominos, and DHL. Most of these deliveries tend to employ bulky drone platforms designed for long-range dispatch and require designated take-off and landing spaces. Additionally, the delivery drones used by logistics companies have limited capabilities to deliver parcels of different sizes. Specifically, they are unable to deliver super-sized parcels (parcels larger than the drone itself) due to parcel position beneath the propeller plane. Placing any object in the slipstream directly under the propellers of the drone generates significant drag that reduces the lifting capability of the drone.

Thus, the standard practice of delivery drones is to place a parcel between and beneath the rotor plane to ensure the slipstream is unblocked.

However, this approach limits the dimensions of parcels that can be delivered. To deliver larger parcels, logistics companies require larger vehicles, regardless of parcel weight, which is expensive and inefficient. Large drones incur a high operational cost as their airframes are heavier and generate more drag. Additional major drawbacks include occupying large storage spaces, reduced portability, reduced functionality in cluttered environments, and the need for designated take-off and landing spaces. A portable, small-sized drone capable of carrying packages larger than its propeller footprint would reduce the need for larger drones.

A possible approach to delivering super-sized parcels is to use drones with adaptive morphology [3]. The foldable scissor-like mechanisms presented in [4], [5], which varies the size of the quadcopter, could be used for accommodating different parcel sizes. However, using adaptive morphology will still not completely remove the restriction on the maximum parcel size. Another approach is to suspend the parcel from the drone with a very long cable [6], [7], which would not interfere with the propeller slipstream because the parcel is far from the downwash of the propellers. However, this approach has two drawbacks: the first is that the cable may become entangled with obstacles, which would prevent the drone from operating in cluttered environments; the second is that the swinging motion of the parcel induced by wind gusts or abrupt maneuvers could destabilize the vehicle and lead to energetically expensive flight adjustments or even a crash. Furthermore, the complexity in the control algorithms to prevent cargo swinging [8]–[10] make cable-suspended load delivery difficult.

We present a novel approach to delivering super-sized parcels, where the parcel is positioned above and within proximity of the propellers (Fig. 1). The approach capitalizes on the different airflow dynamics below (Fig. 2(a)) and above (Fig. 2(b)) the propellers, which eliminates slipstream drag (Fig. 2(a) and 2(b)). However, placing a parcel above a quadcopter encounters two main challenges. The first is CG placement. The CG should be located as close as possible to the propeller plane to reduce

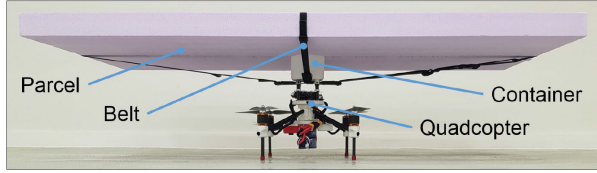


Fig. 1. Quadcopter with a small footprint to deliver parcels of varying sizes. The parcel, a Styrofoam block ( $100 \times 50 \times 5.5$  cm), is placed 15 cm above the propeller plane and is secured to the platform using polyester belts.

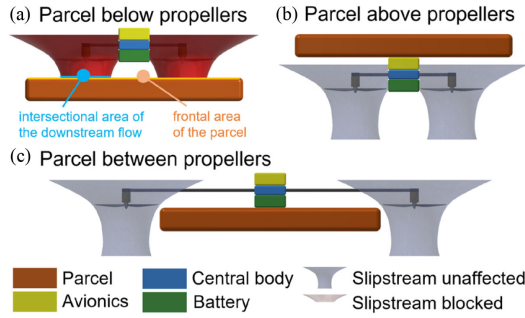


Fig. 2. Side views of quadcopters with parcels placed in different positions. The propeller slipstreams are depicted in grey (the unaffected slipstream) and red (the blocked propeller slipstream). (a) A super-sized parcel placed below propellers creates slipstream drag, which limits lift and flight capability. (b) A parcel placed above, but close to the propellers does not reduce lift as much compared to the parcel placed beneath propellers. (c) A parcel placed between the propellers does not affect lift but restricts the size of a parcel.

control effort of the drone. This is true whether there is a parcel onboard or not and regardless of parcel weight. The vehicle design needs to cover this wide range of mass distributions. The second challenge is to minimize the distance between the propeller plane, and the parcel to minimize the aerodynamic influence of the parcel. In this letter, we developed and validated a quadcopter design that allows its CG to be located near its propellers and the parcel placed at an optimal position above the propellers, determined through physical experiments. In this approach, the propellers can be positioned closer to one another, as they do not need to extend beyond the parcel edges (Fig. 2(c)). Having the propellers closer to one another results in smaller sized quadcopters that are properly sized for the package weight resulting in better portability and storage. This new approach of re-positioning the parcel above the propellers (Fig. 2(b)) eliminates the limitation on parcel size, while maintaining low storage requirements and high portability of the drone (Fig. 1). [11]. The small drone size also allows delivery to cluttered and hard to reach areas that are not accessible for drones that carry parcels placed between the propellers. Finally, this approach contains all the vehicle structure in a small space, limiting the risk of entanglement and complex control algorithms encountered by cable-suspended methods.

## II. BENEFITS OF PLACING A PARCEL ABOVE THE PROPELLERS

Placing a parcel above a quadcopter allows using a smaller footprint drone. This approach brings a number of advantages, which are described in this section.

### A. Space Savings

The footprint size of any quadcopter is a function of propeller size. However, when placing a parcel between the propellers,

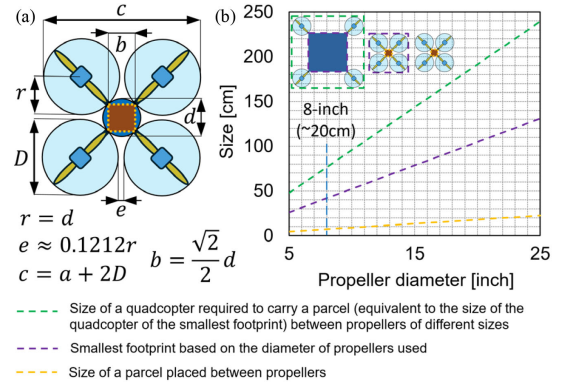


Fig. 3. (a) A schematic representation of the geometric relationship between the radius of the propeller disk  $r$ , diameter  $d$  of the central free space (dark blue circle) between propellers and space between propellers' tips  $e$ . (b) A plot presenting the relationship between propellers diameter and the size of a parcel or quadcopters.

footprint size is also a function of parcel size. The proposed approach of placing the parcel above the propellers decouples arm length from parcel size, which in turn enables significant reduction of the drone's size by ensuring that footprint size is only limited by propeller size. Propeller size is useful to compare the parcel placement approaches because the relations presented here are independent of payload mass.

To study this space reduction, a simple geometric correlation between the propeller size (light blue circles in Fig. 3(a)) and the region enclosed by the four propellers is used (dark blue circle in Fig. 3(a)). The diameter  $d$  of this region is the same as the radius of the propeller disk  $r$ . This configuration includes a small gap  $e$  (12% of  $r$ ) between the propellers tips to prevent contact between the propellers, representing a practical lower limit to vehicle size. A square (brown in Fig. 3(a)) inscribed in the reference circle represents the maximum deliverable size of a square parcel using the conventional approach of placing the parcel between the propellers.

Following these geometric relations, we first identify the largest sized parcel that can be delivered by a vehicle between its propellers (yellow line in Fig. 3(b)). For example, a quadcopter with 8-inch (20.32 cm) propellers has a minimum footprint of  $42 \times 42$  cm (intersection of blue and purple line in Fig. 3(b)). The maximum square-shaped parcel size that can be placed between the propellers measures only  $7 \times 7$  cm (intersection of blue and yellow lines in Fig. 3(b)), regardless of parcel weight. By comparison, a parcel placed above the propeller plane has no restrictions on parcel size. Therefore, the propellers can be placed closer together, resulting in a smaller vehicle footprint (purple line in Fig. 3(b)) for a given propeller size. As a second example, take a parcel with a size of  $42 \times 42$  cm (the threshold of super-sized parcels in the previous example) delivered by placing it between the propellers. The minimum required size of the quadcopter will be  $76.5 \times 76.5$  cm (intersection of blue and green lines in Fig. 3(b)). When compared to the minimum vehicle size for this propeller, there is a volume saving of 70% when placing the parcel above the propellers.

### B. Weight and Drag Savings

A rigid and stable positioning of the propulsion systems is required for efficient flight. Big parcels placed between the propellers requires big quadcopter airframes. Instead, when

the parcel is located above the propellers, the smaller vehicle footprint has comparatively lower mass and drag. To compare the weight and drag between the two approaches, we adopted a simple drone design framework using tube structures.

The tube structures used for the quadcopter's arms are lengthened accordingly to accommodate the different parcel sizes. However, as the lengths of the arms are increased, the tube's thickness and/or diameter has to be increased to maintain the rigidity of the drone's arms. This leads to an increase in both mass and drag incurred by the airframe.

The mass of the tube arm  $M_{tube}$  is computed as

$$M_{tube} = l \cdot \rho_{material} \cdot A_{tube} \quad (1)$$

where  $l$ , is the length of the tube arm,  $\rho_{material}$  is the density of the material used. The cross-sectional area of the tube arm,  $A_{tube}$ , is calculated as

$$A_{tube} = \frac{\pi \cdot (D_{tube\ external}^2 - d_{tube\ internal}^2)}{4} \quad (2)$$

where  $D_{tube\ external}$  is the external diameter of the tube,  $d_{tube\ internal}$  is the internal diameter of the tube. Using the cross-sectional area of the tube, the moment of inertia of the section of the tube  $J$  is calculated as

$$J = \frac{A_{tube}}{16} \quad (3)$$

The deflection of the arm/tube can then be calculated as

$$y_{arm} = \frac{F_{\max.\ thrust} \cdot l^3}{3 \cdot E \cdot J} \quad (4)$$

where  $F_{\max.\ thrust}$  is the force applied (max thrust generated by the motor and propeller), and  $E$  is the Young's modulus. By combining the above expressions, the external diameter of the tube/arm  $D$  can be expressed as

$$D = \sqrt{\frac{64 \cdot F_{\max.\ thrust} \cdot l^3}{3 \cdot E \cdot \pi \cdot y_{arm}} + d^2} \quad (5)$$

By using this expression in equations (1) and (2),  $M_{tube}$  can be described as follows:

$$M_{tube} = \frac{16 \cdot F_{\max.\ thrust} \cdot l^4 \cdot \rho}{3 \cdot E \cdot y_{arm}} \quad (6)$$

Thus,

$$M_{tube} \propto l^4 \quad (7)$$

This indicates that scaling the arm length up exponentially increases the weight of the vehicle. Conversely, a small reduction in arm length dramatically reduces the vehicle weight. A similar analysis can be done with the drag force incurred by the airframe,

$$F_{D_{frame}} = \frac{1}{2} \cdot \rho_{air} \cdot A_{arm\ frontal\ area} \cdot C_{D_{tube}} \cdot V_{cruise}^2 \quad (8)$$

where  $\rho_{air}$  is the density of the air,  $C_{D_{tube}}$  is the drag coefficient of a tube, and  $V_{cruise}$  is the velocity of the drone in cruise flight.  $A_{arm\ frontal\ area}$  is the frontal area of the tube used and can be defined as

$$A_{arm\ frontal\ area} = D \cdot l \quad (9)$$

By combining equations (5), (8), and (9), the following expression is obtained

$$F_{D_{frame}} \propto l^{\frac{5}{2}} \quad (10)$$

This shows a similar exponential increase in drag of the vehicle as a function of arm length, reinforcing the benefits of using a small vehicle, which can only be achieved by placing the parcel above the propellers.

TABLE I  
VALUES USED FOR EQUATION (11). RESULTS OF CALCULATIONS ARE PRESENTED IN TABLE II

| Parameter | $d$  | $v$    | $g$  | $\eta$ | $r_{big\ drone}$ | $r_{small\ drone}$ | $P$ |
|-----------|------|--------|------|--------|------------------|--------------------|-----|
| Values    | 2    | 45     | 9.81 | 0.5    | 3                | 7                  | 0.1 |
| Unit      | [km] | [km/h] | N    | -      | -                | -                  | kW  |

TABLE II  
COMPARISON OF POWER CONSUMPTION OF QUADCOPTERS WITH DIFFERENT PAYLOADS AND MASSES FOR THE 2 km FLIGHT DISTANCE

| Parameter | $M_{payload}$ | $M_{vehicle}$ | Energy       |
|-----------|---------------|---------------|--------------|
|           | 2             | 8             | <b>0.041</b> |
| Values    | 0.5           | 8             | <b>0.035</b> |
|           | 0.5           | 2             | <b>0.008</b> |
| Unit      | [kg]          | [kg]          | [kWh]        |

### C. Power Savings

Using large drones designed for lifting large payloads results in higher operating costs when delivering small and/or lightweight parcels. To illustrate the difference in power consumption of a quadcopter with different payloads, equation (11) from [1] is used:

$$Energy\ (kWh) = \frac{d_{cruise}}{V_{cruise}} \cdot \left( \frac{(m_p + m_v) \cdot V_{cruise}}{\frac{3600}{g} \eta \cdot r} + p \right) \quad (11)$$

where  $d_{cruise}$  is the distance flown,  $m_p$  is the payload mass,  $m_v$  is the vehicle mass,  $V_{cruise}$  is the cruise speed,  $g$  is the gravitational acceleration,  $\eta$  is the motor/propeller power transfer efficiency,  $r$  is the lift/drag ratio, and  $p$  is the power consumption of electronics.

An example is presented in Tables I and II based on quadcopters from [1], [12]. A quadcopter weighing 8 kg that transports a 2 kg payload over a 2 km range consumes 0.041 kWh of energy (the quadcopter in [1]). Based on equation (11), the same quadcopter carrying a 75% lighter payload (0.5 kg) still consumes 96% of the original energy. However, for the same 0.5 kg payload, a smaller quadcopter (similar to the quadcopter in [12]) weighing 2 kg consumes only 0.008 kWh over the 2 km range, which translates to a 76.4% decrease in energy compared to the larger vehicle. These calculations suggest that using a small drone to transport lightweight yet large parcels is more efficient and economical than using larger sized and heavier drones.

### III. DEGRADATION OF LIFT FORCE DUE TO PARCEL PLACEMENT

In this section, discussion of the aerodynamic challenges associated with different parcel positions are presented. First consider the case where a parcel is placed below the propellers. When the airflow produced by a propeller encounters an object rigidly fixed to the same structure as the propulsion system, the slipstream drag force generated by the object opposes the thrust force, thus reducing the multicopter's capability to fly (Fig. 4(a)). In this case, the lift can be calculated from:

$$L = T - F_{SD} \quad (12)$$

where  $L$  is the lift force,  $T$  is the thrust generated by the propeller, and  $F_{SD}$  is the slipstream drag force acting on the parcel. The

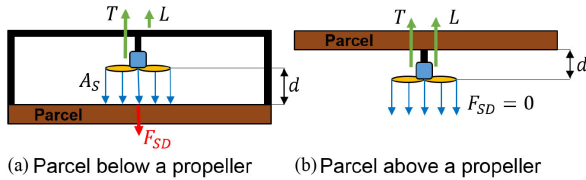


Fig. 4. Representation of the distribution of forces. (A) Parcel placed below the propeller produces the slipstream drag-force  $F_{SD}$  (red arrow) that opposes the thrust force  $T$  (left green arrow). Thus, the lift  $L$  (right green arrow) is reduced.  $A_S$  is the cross-sectional area of the parcel within the propeller wash  $d$  between propeller and the parcel. (B) Parcel placed above the propeller does not generate as much drag, thus does not reduce lift.

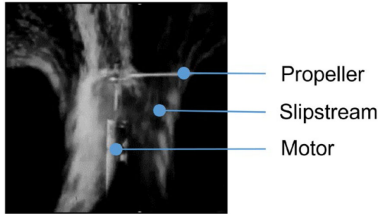


Fig. 5. Screen shot from an experimental representation video of the flow distribution adapted from [12].

slipstream drag-force is dependent on the distance  $d$  between propeller and the parcel and can be described as:

$$F_{SD} = f(d, \rho_{air}, A_S, C_{SD}, V_{RPM}) \quad (13)$$

where,  $A_S$  is the cross-sectional area of the parcel within the propeller wash as shown in Fig. 4(a),  $C_{SD}$  is the slipstream drag coefficient of the parcel, and  $V_{RPM}$  is the velocity of the airstream at the point of contact with the parcel as a function of rotation speed of propeller. The slipstream drag force is not dependent on the entire frontal area of the parcel, but rather the intersectional area of the flow below the propeller and the parcel (Fig. 4(a)). As presented in Fig. 5 [13], the slipstream below the propeller is more defined, condensed, and narrow than above the propeller.

Next, consider the case of the parcel placed above the propellers. With the parcel placed above the propellers, the slipstream is not blocked, and therefore slipstream drag is eliminated. However, a challenge associated with this approach is that an object placed above, but in close proximity to the propellers will hinder airflow into the propellers. According to Froude's momentum theory of propulsion [14], the air passing through the rotor disc plane receives energy from the propeller, thus generating thrust. However, when there is insufficient airflow to the propeller, a lower amount of energy is transferred to the air, reducing the thrust produced. Instead of blocking the airflow below the propellers, placing the parcel above blocks airflow above the propellers (Fig. 4(b)). Mathematically, this is written by replacing slipstream drag in equation (12) with inflow blockage. To prevent inflow blockage, the parcel placed above the propellers has to be located at a distance that provides sufficient room for airflow to the propellers. Because the airflow above the propeller is wider than below, it is possible to place parcels mounted above the propellers closer to the propellers than if they were mounted below (Fig. 2(b)). Furthermore, because the airflow above the propeller is independent of flow direction, parcels placed above the propellers are not limited in size, unlike parcels placed between the propellers (Fig. 2(c)).

The aerodynamic requirements of our approach are validated through physical experiments, comparing slipstream drag and inflow blockage effect, in Sections V and VI.

In this letter, the influence of parcel position on lift was only studied in hovering flight. This is because the additional drag during cruise flight is independent of parcel position, and this subject is covered in separate studies [15], [16].

It is important to highlight that the parcel position might affect the induced moments due to the aerodynamic forces on the parcel during cruise flight, which may influence power consumption.

#### IV. CONFLICTING CONSTRAINTS OF CG LOCATION AND EFFICIENT AERODYNAMICS

Multicopters are naturally unstable platforms, thus a quadcopter requires a controller to stabilize itself regardless of the location of center of gravity (CG) and position of parcel [17], [22]. However, to reduce the quadcopter's control effort, the CG of the entire platform should be as close to the propeller plane as possible [17]. Additionally, Pounds et.al. concluded that the CG should lie close to, but slightly above the propeller plane for the best disturbance rejection [18]. This preference is further supported in [19], which stated that quadcopters under a proportional-integral-derivative (PID) controller are more stable when the load is placed directly on top of the airframe, especially for robotic payload carrying tasks [20]. Moreover, the PID controller can handle CG offset from the yaw axis more easily by when the CG is placed above the propeller plane. This is particularly important for parcel delivery, as the parcel CG may not be centered in the parcel.

It is ideal to place the parcel as close as possible to the propeller plane to keep the CG as close as possible to the propeller plane. However, placing a parcel close to the propellers will block the airflow stream into the propellers, due to inflow blockage effect. Thus, to address the problem of competing constraints it is necessary to find the smallest distance between the parcel and the propellers that does not inhibit adequate airflow. This was studied experimentally in Sections V and VI. Additionally, distance of the CG from the propellers' plane can vary significantly with and without a parcel. To keep the smallest distance between the CG and the propeller's plane in both configurations, a quadcopter was designed (see Section VI) to situate the propeller plane midway between the two CG locations.

#### V. EXPERIMENTAL VALIDATION-SINGLE PROPELLER

To demonstrate the aerodynamic effects of parcel position on the drone, a series of experiments were performed. These experiments were conducted to demonstrate that slipstream drag reduces lift more than inflow blockage does. During the experiments, lift, slipstream drag, and electric power consumption were measured at different distances  $d$  between a parcel and a single propeller (Fig. 6(a-c)).

Two configurations were considered, one with the parcel below the propeller (Fig. 6(a)) and another with the parcel above the propeller (Fig. 6(c)). Additionally, for each configuration, two other factors were considered:

- i) dependency of lift on different rotation speeds;
- ii) dependency of lift on different propeller diameters. The first experiment was conducted with an APC  $8 \times 4.5$  propeller and the second at a constant 9000RPM, which is 70% of the

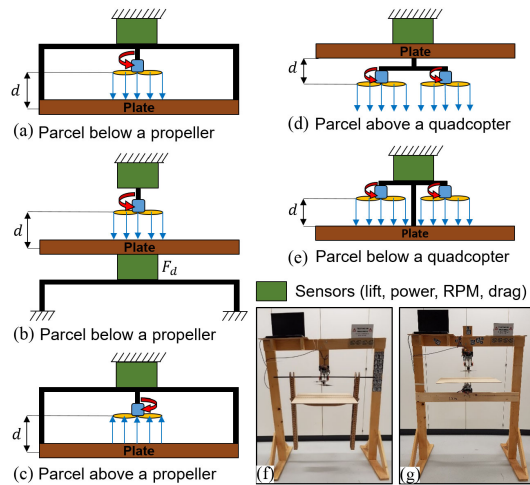


Fig. 6. (a-c) Schematic representation of the experimental set-up for lift and drag measurements with a single propeller. The blue arrows represent the direction of the airflow. The red arrows represent the direction of the rotation of propellers. (a) Plate placed below the propeller. (b) Plate placed below the propeller. Different sizes of plates are fixed to the bottom sensor. (c) Plate placed above the propeller. (d-e) The schematic representation of the experimental set-up for lift and drag measurements with a quad configuration. (d) Quadcopter with a plate placed above the propellers. (e) Quadcopter with a plate placed below the propellers. (f) Photograph of the setup with a plate of size  $60 \times 60$  cm. (g) Photograph of the setup to measure the slipstream drag force when the plate is placed below the propellers.

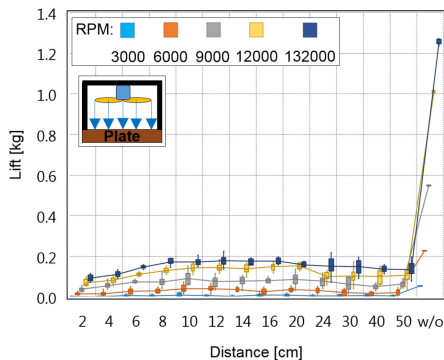


Fig. 7. Influence of the distance of the plate below the propeller on lift measurements. The plot presents lift measurements of APC MR8x4.5 propeller with a flat plate (the equivalent of a parcel) placed beneath the propellers for different rotation speeds.

maximum rotation speed of the propeller-motor pair used in the first experiment. This value was chosen because multicopters do not cruise at maximum throttle but rather around 70% (9000 RPM for proposed setup) capability.

To represent the parcel, a flat wooden MDF plate  $60 \times 60 \times 0.5$  cm was attached to a force sensor (marked as a green rectangle in Fig. 6(a)) via a vertical wooden structure connected to a horizontal 10 mm carbon tube (both marked as black beams in Figs. 6A and 7C). The distance between the MDF plate and the propeller can be varied from 2 cm to 50 cm. A control case was also run without the MDF plate. The motor is powered by a power supply (Keithley 2260B-30-72) which has a maximum output of 720 W.

The measurements were conducted using the RC Benchmark 1580 Series dynamometer sensor (Fig. 6, marked as a green rectangle) [23] attached to a stand. The motor used for the tests was an AXI 2217-16 V2 (1380 KV) with a 40A ESC (Electronic

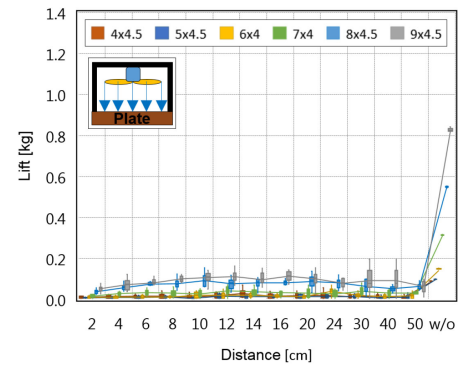


Fig. 8. Influence of the distance of plate below the propeller on lift measurements. Measurements are obtained at a constant speed of 9000 RPM. Propellers of various diameters but similar pitches were used.

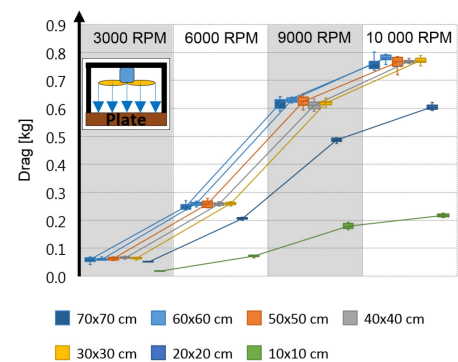


Fig. 9. Drag measurements of different sized square plates placed 10 cm below a single propeller.

Speed Controller). The voltage was set to 12.6 V which is equivalent to a fully charged 3S battery. Each measurement was done ten times.

### A. Parcel Below the Propeller

When the parcel (MDF plate) was positioned directly below the propeller, the slipstream drag significantly reduced the lift as observed in Figs. 7 and 8. Regardless of rotation speed, shown in Fig. 7, or propeller diameter, in Fig. 8 the observed effect of parcel placement on lift is the same. A plate situated as far as 50 cm beneath the propeller still diminishes the measured lift by 90% compared to when there is no plate at all (marked “w/o”—without, on the farthest right in both plots). This shows that there is no dependency on distance between the propeller and plate regardless of rotation speed or propeller size.

Experimental verification that slipstream drag is a function of the area of the parcel in contact with the propeller slipstream  $A_S$  was also performed. Different sized square plates were attached to the dynamometer sensor and were placed 10 cm below the propeller (Figs. 6B and (g)). As expected, plates that are larger (30 cm and above) than the propeller disk have approximately the same drag measurements, regardless of how much larger they are (Fig. 9). This is because the cross-sectional area between the slipstream and parcel is constant between runs. When the plate is equivalent to or smaller than the propeller disk, the measured drag force is lower and varies with the size of the plate. These results confirm that the slipstream drag is indeed dependent on the area of the parcel in contact with the propeller slipstream.

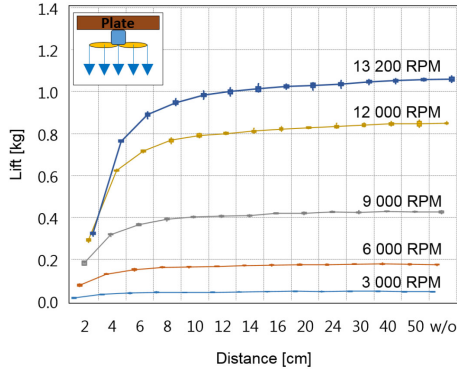


Fig. 10. Influence of the distance of the plate above the propeller on lift measurements. The plot presents lift measurements of APC MR8x4.5 propeller with a flat plate (the equivalent of a parcel) placed above the propellers for different rotation speeds.

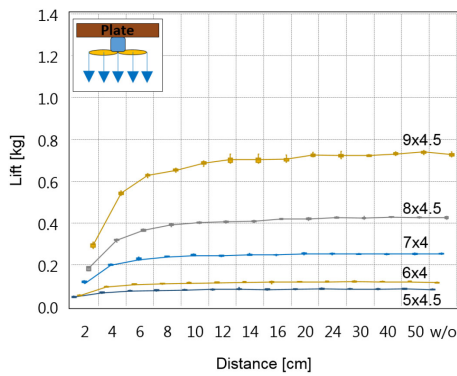


Fig. 11. Influence of the distance of plate above the propeller on lift measurements. Measurements are obtained at a constant speed of 9000 RPM. Propellers of various diameters but similar pitches were used.

### B. Parcel Above the Propeller

Conducting the experiment with the parcel above the propellers illustrated that the inflow blockage is most significant when the parcel is within 10 cm of the propeller (Fig. 10). Beyond 10 cm, as the distance between the propeller and parcel increases, the lift levels off and becomes constant, within 10% of its maximum value. Within the 10 cm distance, the most significant impact on the lift is the plate placed 2 cm above the propeller. At 12000 RPM, the lift is affected by 57% while at 13200 RPM, the lift is affected by 66%.

As with the previous experiment, the investigation of different sized propellers (Fig. 11) was conducted at 9000 RPM. The lift stabilizes at 6 to 12 cm distance between the plate and the propellers for each of the propeller sizes. This matches well with the 10 cm threshold found when varying the RPM. Larger propellers have larger volumes of air inflow, therefore with larger inflow blockage, there is a larger decrease in lift. This is why the initial slopes are steeper for the larger propellers. In the experiments with the plate placed above the propeller (Figs. 10 and 11), the distance at which the lift begins to converge within 10% of its maximum value for a specific propeller is approximately equivalent to its radius, which is significantly less than 90% when a parcel is placed below the propeller.

Throughout the experiments, the electrical power consumption was measured. Analyzed data (Table III) suggest that the electric power consumption remained constant as the plate was

TABLE III  
ELECTRIC POWER CONSUMPTION OF MOTOR FOR DIFFERENT PROPELLER SIZES

| Parameter | Propeller size | Average electric power [W] |                         |
|-----------|----------------|----------------------------|-------------------------|
|           |                | Parcel above propellers    | Parcel below propellers |
| Values    | 4              | 19.0 ± 0.2                 | 20.8 ± 0.1              |
|           | 5              | 28.4 ± 0.2                 | 28.0 ± 0.2              |
|           | 6              | 31.5 ± 0.2                 | 30.1 ± 0.3              |
|           | 7              | 54.6 ± 0.4                 | 56.0 ± 0.4              |
|           | 8              | 103.3 ± 1.1                | 104.3 ± 0.5             |
|           | 9              | 162.1 ± 2.5                | 165.0 ± 1.3             |
| Unit      | [inch]         | [W]                        | [W]                     |

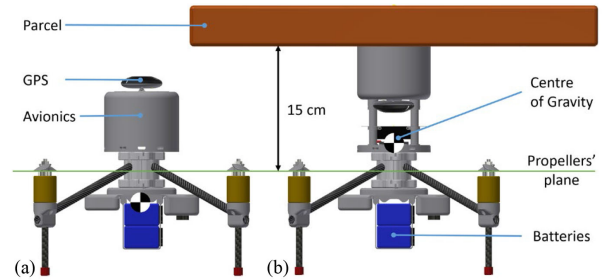


Fig. 12. Side views of the quadcopter. (a) The quadcopter without a parcel. Center of Gravity placed 36 mm below the plane of the propellers along the yaw axis. (b) The drone with a parcel placed above the propellers. The Center of Gravity was placed 39 mm above the propeller plane along the yaw axis.

moved away from a propeller for parcel placements above and below the propeller. This is indicated by the small corresponding standard deviation values in Table III.

## VI. EXPERIMENTAL VALIDATION—DELIVERY DRONE

To validate the concept of delivering super-sized parcels, a  $50 \times 50$  cm quadcopter that can carry 0.75 kg worth of payload was designed and manufactured (Figs. 1 and 12).

### A. Delivery Drone Description

The proposed design ensures that the CG is positioned close to the propeller plane with or without the payload. With the payload, the CG is designed to be above the propellers to ensure that the PID controller handles potential parcel CG offsets from the yaw axis efficiently. Without the payload, the CG will subsequently be located below the propellers. If the payload is lighter than a maximum 0.75 kg, the CG is located above but closer to the propeller plane. This positioning of CG allows to reduce control effort as discussed in Section IV.

To position the CG close to the propeller plane, batteries are located below the propeller plane while the parcel is placed above the propeller plane. More importantly, to achieve a similar distance between the CG and the propeller plane with and without a parcel, the quadcopter arms are inclined by 68 degrees to the yaw axis (Fig. 12). This shifts the propeller plane to the midway point between the extreme CG positions. In the proposed design, the parcel is positioned 15 cm above the propeller plane as this is above the distance that minimally affects the lifting capability of the propulsion system with a margin of safety.

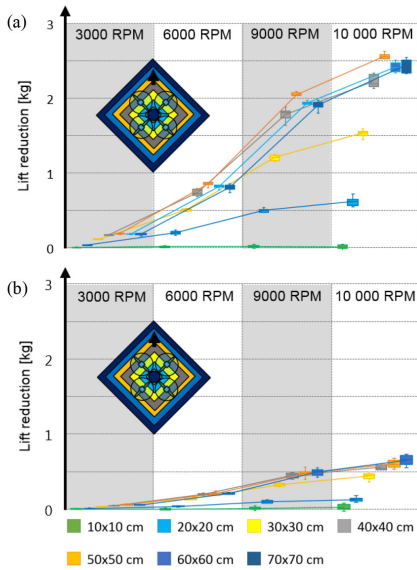


Fig. 13. (a) Lift measurements based on different sizes of square plates placed 10 cm above a quadcopter. The size of the quadcopter is  $50 \times 50$  cm. (b) Lift measurements based on different sizes of square plates placed 10 cm below a quadcopter. The size of the quadcopter is  $50 \times 50$  cm. Colors of the squares correspond to the different sized plates. The total lift is 0.20 kg, 0.89 kg, 2.11 kg, and 2.66 kg for 3000 RPM, 6000 RPM, 9000 RPM, and 10000 RPM respectively.

The parcel is secured to the top of the drone by two polyester belts crossed perpendicular to each other (Fig. 1). A GPS module is connected to one of the belts and when strapped, is situated above the box. This is favorable as GPS readings can be affected by objects, such as parcels, made of or containing metal material (e.g. aluminum foil). The platform is equipped with four AXI 2217-16 V2 (1380 KV) motors with APC8x4.5 propellers and 4in1 ESC. The flight controller used is PixHawk 4 Mini. The drone is equipped with two 3S Li-Po batteries, each 5000 mAh.

### B. Influence of a Parcel on a Quadcopter Propulsion System

The influence of parcel size on the lifting capability of the quadcopter was investigated by attaching different sizes of square plates to the quadcopter as shown in Fig. 6(d-e). These plates range from  $10 \times 10$  cm to  $70 \times 70$  cm, attached at a 10 cm distance from the propellers, as concluded earlier that the distance between the parcel and the propeller should be equal to the radius of the propeller used.

Two experiments were conducted using the previously described dynamometer setup, the first with the parcel placed above and the second with the parcel placed below the propellers (Fig 6D-E). In both cases, ten measurements of lift were made for four rotation speeds. The lift reduction is presented in Fig. 13. It was calculated by subtracting the measured lift with a parcel from the measured lift without the parcel. Thus, the plots show directly the amount of lift reduction for each plate.

The schematic representation of how the plate was attached below the quadcopter is presented in Fig. 6(e). The results of the experiment are presented in Fig. 13(a) and show that a plate bigger than the enclosed area between the propellers has significant influence on lift reduction. For instance, plates of sizes  $70 \times 70$  cm and  $60 \times 60$  cm encountered up to 96% lift reduction for 10000RPM which is the equivalent of 2.4 kg of lift. Also of note is that a higher inflow blockage was measured

with a plate of same size as the quadcopter than a larger plate than the quadcopter. This is likely due to vortices at the edge of the plate. Further investigations are required to understand this phenomenon.

In Fig. 13(b), results of the lift reduction are presented for a parcel placed above the propeller plane. The lift reduction between different sized parcels is very small for small rotation speeds. When the speed increases, the lift reduction increases with increase in size of the propellers. The experiments with a small parcel ( $10 \times 10$  cm and  $20 \times 20$  cm) below the propeller plane confirm that a smaller parcel size has smaller influence on the lift. This is not true of larger parcels, that confirms that the arms of the multicopter have to be increased to secure unobstructed airflow. The earlier experiment on a single propeller spinning at 9000RPM showed that a  $60 \times 60$  cm parcel placed 10 cm above produces only a 6% lift reduction (Fig. 7). However, when the same sized plate is placed 10 cm above the quadcopter's propellers, a maximum lift reduction due to inflow blockage of about 23.4% is measured (Fig. 13(b)). This is approximately four times the reduction with a single propeller, suggesting that inflow blockage is additive with the number of propellers. Repositioning the parcel to 15 cm above the quadcopter further decreases the lift reduction to 14%. This is a remarkable improvement compared to the 96% lift reduction due to slipstream drag if the parcel is placed 15 cm below the quadcopter.

The phenomena shown in this experiment, that attaching a flat object above or below propellers differs from the ceiling effect [24]–[27] or the ground effect [28]–[30]. This is because unlike the ceiling or the ground, the parcel is rigidly connected to the airframe. Because of this rigid connection, the force produced by the motors is internal to the system and hence cannot affect the dynamics of the system as a whole. In the ceiling effect, the ceiling is not part of the system, thus the force created by the motors is external. Both the ceiling effect and inflow blockage result in a greater pressure difference across the rotor disk increasing thrust. However, with the ceiling effect, the drone is sucked up into the ceiling. The rigid connection between the parcel and motors prevents the vehicle being sucked up to the parcel. In Figs. 10 and 11, the observed effect is the opposite of the ceiling or ground effects; the closer the parcel is to the propeller the smaller lift is.

### C. Flight Experiments

Flight tests with the quadcopter in hover were performed to validate the approach of placing the parcel above the propeller plane while minimally affecting its lifting capabilities. A flat plate was attached above the propellers at a distance of 15 cm from the propeller plane. During the experiment, the quadcopter employed 55% (550g payload) throttle with an ultrasound sensor to maintain an altitude of 1.5 m above the ground. The drone used a standard PX4 flight stack software for the  $\times$  shaped quadcopter, which is much simpler than the complex controllers used when delivering a parcel on a long tether. A pilot kept its position constant. The drone automatically landed after reaching 5% of its battery level. All flight tests were performed three times and the average time of hover is reported. The first experiments were the quadcopter with a super-sized foam plate and smaller box, both placed 15 cm above the propellers. The experiment showed a difference of 2 minutes in the hover flight time (12%) between flight with a super-sized parcel and a smaller parcel of

the same weight, both placed above the quadcopter. The foam plate measured  $100 \times 50 \times 5.5$  cm and had a mass of 550 g. Its time of hover was 15 minutes 30 seconds. The smaller parcel measured  $7 \times 7 \times 5$  cm also had a mass of 550 grams. Its time of hover was 17 minutes 30 seconds. The experiment was repeated with the parcel placed below the propellers. The time of hover with the smaller parcel (550 g) attached between the propellers was 16 minutes 10 seconds. The super-sized parcel attached 12.5 cm below the propeller plane generated excessive drag, which counteracted all of the thrust generated. As such, the drone was not able to take-off (see included video).

## VII. CONCLUSION

This letter presented the novel concept of placing a parcel above the propeller plane of a quadcopter. This approach allows the transportation of different sized parcels without limitation, unlike when a parcel is beneath the frame of the quadcopter. Placing a parcel above the propellers enables a smaller footprint of the quadcopter, reducing the airframe's size, weight and drag, and enhancing its storage and transportation capabilities. Moreover, a smaller drone is more feasible for deliveries in cluttered environments. Simply relocating the package brings these benefits without the use of exotic designs or a complex controller, a simple PID can be used.

We validated the proposed approach, by developing and testing a quadcopter that allows for the transportation of different sized parcels, including super-sized parcels that are larger than the quadcopter itself. Experiments revealed that placing a parcel above the quadcopter at a distance equivalent to the radius of the operating propeller, reduces the drone's lifting capability by 23%, compared to 96% when the parcel is below the quadcopter. When the distance between the quadcopter and parcel placed above it is increased, the lift reduction can be further reduced.

The new approach of placing a parcel above the propeller plane should spur the development of new cargo delivery drone designs capitalizing on the compactness, efficiency and functionality of the strategic parcel placement. Future work will be focused on the design of a compact protective cage around the propellers [31] and investigating the influence of parcel size on the drone's cruise performance.

## ACKNOWLEDGMENT

The authors would like to acknowledge Cameron Dowd for manufacturing the test bench and Hauke Maack for help in designing part of the prototype drone.

## REFERENCES

- [1] R. D'Andrea, "Guest editorial can drones deliver?" *IEEE Trans. Autom. Sci. Eng.*, vol. 11, no. 3, pp. 647–648, Jul. 2014.
- [2] D. Floreano and R. J. Wood, "Science, technol. and the future of small autonomy drones," *Nature*, vol. 521, no. 7553, pp. 460–466, 2015.
- [3] S. Mintchev and D. Floreano, "Adaptive morphology: A design principle for multimodal and multifunctional robots," *IEEE Robot. Autom. Mag.*, vol. 23, no. 3, pp. 42–54, Sep. 2016.
- [4] N. Zhao, Y. Luo, H. Deng, and Y. Shen, "The deformable quad-rotor: Design, kinematics and dynamics characterization and flight performance validation," in *Proc. IEEE Int. Conf. Intell. Robots Syst.*, 2017, pp. 2391–2396.
- [5] D. Falanga, K. Kleber, S. Mintchev, D. Floreano, and D. Scaramuzza, "The foldable drone: A morphing quadrotor that can squeeze and fly," *IEEE Robot. Autom. Lett.*, vol. 4, no. 2, pp. 209–216, Apr. 2019.
- [6] M. Bernard, K. Kondak, I. Maza, and A. Ollero, "Autonomous transportation and deployment with aerial robots for search and rescue missions," *J. F. Robot.*, vol. 28, no. 6, pp. 914–931, 2011.
- [7] I. Maza, K. Kondak, M. Bernard, and A. Ollero, "Multi-UAV cooperation and control for load transportation and deployment," *J. Intell. Robot. Syst.: Theory Appl.*, vol. 57, no. 1–4, pp. 417–449, 2010.
- [8] K. Sreenath, N. Michael, and V. Kumar, "Trajectory generation and control of a quadrotor with a cable-suspended load - A differentially-flat hybrid system," in *Proc. IEEE Int. Conf. Robot. Autom.*, 2013, pp. 4888–4895.
- [9] K. Sreenath, T. Lee, and V. Kumar, "Geometric control and differential flatness of a quadrotor UAV with a cable-suspended load," in *Proc. IEEE Conf. Decis. Control*, 2013, pp. 2269–2274.
- [10] S. Tang, V. Wuest, and V. Kumar, "Aggressive flight with suspended payloads using vision-based control," *IEEE Robot. Autom. Lett.*, vol. 3, no. 2, pp. 1152–1159, Apr. 2018.
- [11] Forbes. Apr. 13, 2019. [Online]. Available: <https://www.forbes.com/sites/jonbird1/2018/07/29/what-a-waste-online-retails-big-packaging-problem/#701084ac371d>
- [12] P. M. Kornatowski, S. Mintchev, and D. Floreano, "An origami-inspired cargo drone," in *Proc. IEEE Int. Conf. Intell. Robots Syst.*, 2017, pp. 6855–6862.
- [13] NASA CRgis. Feb. 10, 2019 "Helicopter test tower, films section: Visualization of vertical flows over propellers," [Online]. Available: <https://crgis.ndc.nasa.gov/historic/1231A>
- [14] E. L. Houghton, *Aerodynamics for Engineering Students*, pp. 527–528, 2016.
- [15] H. Sakamoto and H. Haniu, "Aerodynamic forces acting on two square prisms placed vertically in a turbulent boundary layer," *J. Wind Eng. Ind. Aerodynamics*, vol. 31, no. 1, pp. 41–66, 1988.
- [16] X. Ortiz, D. Rival, and D. Wood, "Forces and moments on flat plates of small aspect ratio with Application to PV wind loads and small wind turbine blades," *Energies*, 2015.
- [17] Q. Quan, *Introduction To Multicopter Design and Control*. Berlin, Germany: Springer, 2017.
- [18] P. Pounds, R. Mahony, and P. Corke, "Modelling and control of a large quadrotor robot," *Control Eng. Practice*, vol. 18, no. 7, pp. 691–699, 2010.
- [19] P. E. I. Pounds, D. R. Bersak, and A. M. Dollar, "Stability of small-scale UAV helicopters and quadrotors with added payload mass under PID control," *Autonomous Robots*, vol. 33, no. 1–2, pp. 129–142, 2012.
- [20] H. N. Nguyen, C. Ha, and D. Lee, "Mechanics, control and internal dynamics of quadrotor tool operation," *Automatica*, vol. 61, pp. 289–301, 2015.
- [21] I. Palunko and R. Fierro, "Adaptive control of a quadrotor with dynamic changes in the center of gravity," *IFAC Proc. Volumes*, 2011, vol. 44, no. 1, PART 1, pp. 2626–2631.
- [22] S. Lee, D. K. Giri, and H. Son, "Modeling and control of quadrotor UAV subject to variations in center of gravity and mass," in *Proc. 14th Int. Conf. Ubiquitous Robots Ambient Intell.*, 2017, pp. 85–90.
- [23] RCbenchmark.com Mar. 24, 2019. [Online]. Available: <https://www.rcbenchmark.com>
- [24] Y. H. Hsiao and P. Chirarattananon, "Ceiling Effects for Surface Locomotion of Small Rotorcraft," in *Proc. IEEE/RSJ Int. Conf. Intell. Robots Syst.*, 2019, pp. 6214–6219.
- [25] P. J. Sanchez-Cuevas, G. Heredia, and A. Ollero, "Multirotor UAS for bridge inspection by contact using the ceiling effect," in *Proc. Int. Conf. Unmanned Aircraft Syst.*, 2017.
- [26] S. A. Conyers, M. J. Rutherford, and K. P. Valavanis, "An empirical evaluation of ground effect for small-scale rotorcraft," in *Proc. IEEE Int. Conf. Robot. Autom.*, 2018.
- [27] A. E. Jimenez-Cano, P. J. Sanchez-Cuevas, P. Grau, A. Ollero, and G. Heredia, "Contact-based bridge inspection multirotors: Design, modeling, and control considering the ceiling effect," *IEEE Robot. Autom. Lett.*, vol. 4, no. 4, pp. 3561–3568, Oct. 2019.
- [28] R. W. Prouty, *Helicopter Performance, Stability, and Control*, Malabar, Florida, 2006.
- [29] P. Sanchez-Cuevas, G. Heredia, and A. Ollero, "Characterization of the aerodynamic ground effect and its influence in multirotor control," *Int. J. Aerospace Eng.*, 2017.
- [30] S. Gao, C. Di Franco, D. Carter, D. Quinn, and N. Bezzo, "Exploiting ground and ceiling effects on autonomous UAV motion planning," in *Proc. Int. Conf. Unmanned Aircraft Syst.*, 2019, pp. 768–777.
- [31] P. M. Kornatowski, M. Feroskhan, W. J. Stewart, and D. Floreano, "A morphing cargo drone for safe flight in proximity of humans," *IEEE Robot. Autom. Lett.*, 2020, doi: [10.1109/LRA.2020.2993757](https://doi.org/10.1109/LRA.2020.2993757).